

Epidemic processes with vaccination and immunity loss studied with the BLUES function method.

Jonas Berx¹ and Joseph O. Indekeu¹

¹*Institute for Theoretical Physics, KU Leuven, B-3001 Leuven, Belgium*

(Dated: July 2, 2021)

Abstract

The BLUES function method is applied to the epidemiological SIRS model with vaccination, described by coupled nonlinear ordinary differential equations. Accurate analytic approximations are obtained for the time evolution of the susceptible and infected population fractions. The results are compared with those obtained with alternative methods, notably Adomian decomposition, variational iteration and homotopy perturbation. In contrast with these methods, the BLUES iteration converges rapidly, globally, and captures the exact asymptotic behaviour for long times. The time of the infection peak is calculated using the BLUES approximants and the results are compared with numerical solutions.

I. INTRODUCTION

Systems of coupled differential equations (DEs) are omnipresent in the sciences, medicine and even in the humanities. While some of these systems have exact closed-form solutions, the majority do not and hence need to be solved by numerical means. One way to supplement direct numerical simulation with useful information about the (physical) structure behind the coupled DEs is to use approximate (semi-)analytical solutions. The best-known examples of methods to calculate such analytical approximants are the Adomian decomposition method (ADM) [1, 2], the variational iteration method (VIM) [3] and the homotopy perturbation method (HPM) [4]. However, a drawback of these methods is the poor convergence for large values of the independent variable (e.g., for long times).

A well-known example of nonlinear coupled DEs is the susceptible-infected-recovered-susceptible (SIRS) model for studying the time-evolution of infectious diseases [5]. There have been attempts to generate approximate solutions for this model using the ADM [6], the VIM and the HPM [7, 8] but these solutions diverge quickly and necessitate an improvement of the methods in order to extend the region of convergence.

This paper is structured as follows: in Section II we extend the by now established BLUES function method [9–12] to a system of nonlinear coupled ordinary DEs. Next, in Section III, we describe the SIRS model with a constant vaccination strategy and reduce the system to the two-dimensional subsystem we subsequently solve. In Section IV we set up the BLUES function method for coupled DEs and apply it, generating approximate solutions to the SIRS model. The results are compared with the numerical solution and with results from three other methods, being the ADM, VIM and HPM. We use the analytical approximants to calculate the time at which the infection peak occurs and compare with numerical results. Finally, in Section V we present the conclusions and an outlook.

II. BLUES FUNCTION METHOD FOR COUPLED DIFFERENTIAL EQUATIONS

Here we extend the BLUES iteration originally developed for ordinary DEs [9–11] and partial DEs [12] to a system of coupled ordinary DEs. The role of the inhomogeneous *source (or sink) term* in the context of the ordinary DE will now be taken over by a vector of

sources (or sinks).

Let us start from an n -dimensional system of inhomogeneous nonlinear coupled ordinary DEs that can be written as a nonlinear operator \mathcal{N}_t acting on a vector $\mathbf{X}(t)$, with source vector $\boldsymbol{\chi}(t)\Theta(t)$, with $\Theta(t)$ the Heaviside step function (which we take to be unity for positive times *including* $t = 0$),

$$\mathcal{N}_t \mathbf{X}(t) = \boldsymbol{\chi}(t), \forall t > 0 \quad (1)$$

and suitable initial conditions for $t = 0$,

$$\mathbf{X}(0) = \mathbf{C}. \quad (2)$$

We now judiciously decompose the nonlinear operator \mathcal{N}_t into a linear operator \mathcal{L}_t , which contains *inter alia* a first derivative in time, and a residual operator \mathcal{R} , i.e., $\mathcal{R} \equiv \mathcal{L}_t - \mathcal{N}_t$, which contains the nonlinear part of \mathcal{N}_t . We add the subscript t to the linear and nonlinear operators to emphasize their dependence on time. In the application we consider in this work, \mathcal{R} does not depend on t . Thus the action of the linear operator on \mathbf{X} results in the following associated linear coupled system

$$\mathcal{L}_t \mathbf{X} = \mathbf{X}_t - A\mathbf{X} = \boldsymbol{\chi}, \forall t > 0 \quad (3)$$

where the subscript denotes derivative w.r.t. time and the same boundary conditions are imposed as in (1). The elements of the matrix A are constants in most of the applications we have in mind. We now propose to rewrite the system of DEs in an equivalent form by incorporating the initial condition through multiplication of \mathbf{C} with a Dirac delta source $\delta(t)$ located at $t = 0$ and by including this term on the right-hand-side of the inhomogeneous system, i.e.,

$$\mathcal{L}_t \mathbf{X} = \mathbf{X}_t - A\mathbf{X} = \boldsymbol{\chi}\Theta + \mathbf{C}\delta \equiv \boldsymbol{\psi}, \forall t \geq 0 \quad (4)$$

where we have combined the external source $\boldsymbol{\chi}\Theta$ and the “initial condition source” $\mathbf{C}\delta$ into the combined source $\boldsymbol{\psi}$. This formulation amounts to reset the initial condition to zero, so that $\mathbf{X}(t) = 0$ for $t \leq 0^-$, followed by a jump in \mathbf{X} implied by integrating the DE over the delta source, so that $\mathbf{X}(0^+) = \mathbf{C}$ and $\mathbf{X}(t)$ evolves in a continuous manner for $t > 0$. The solution of this linear system (4) is the following convolution integral [13, 14]

$$\mathbf{X}(t) = (G * \boldsymbol{\psi})(t) = G(t)\mathbf{C} + \int_{\mathbb{R}} G(t-t')\boldsymbol{\chi}(t')\Theta(t')dt', \quad \forall t > 0 \quad (5)$$

where $G(t)$ is the Green function matrix for the inhomogeneous linear system. This object can be calculated by finding the matrix exponential $\exp(At) \equiv \mathbb{1} + At + \dots$, i.e.,

$$G(t) = e^{At}\Theta(t). \quad (6)$$

This Green function matrix solves the linear system with a delta function unit matrix source, i.e., it is a solution of the matrix equation

$$G_t - AG = \delta(t)\mathbb{1}, \quad \forall t \geq 0. \quad (7)$$

Adopting the BLUES function strategy, a solution to the nonlinear system (1), rewritten in the equivalent form

$$\mathcal{N}_t \mathbf{X} = \boldsymbol{\chi}\Theta + \mathbf{C}\delta \equiv \boldsymbol{\psi}, \quad \forall t \geq 0 \quad (8)$$

is now proposed in the form of a convolution $\mathbf{X}(t) = (B * \boldsymbol{\phi})(t)$, in which the function $B(t)$, named BLUES function, is taken to be equal to the Green function of the chosen related linear system, i.e., $B(t) = G(t)$ and the new source $\boldsymbol{\phi}(t)$ is to be calculated by systematic iteration, using the given (combined) source $\boldsymbol{\psi}(t)$. This procedure starts from the following implicit equation, which makes use of the action of the residual operator,

$$\begin{aligned} \boldsymbol{\phi} &= \boldsymbol{\psi} + (\boldsymbol{\phi} - \boldsymbol{\psi}) \\ &= \boldsymbol{\psi} + \mathcal{R}(B * \boldsymbol{\phi}). \end{aligned} \quad (9)$$

To find the solution to the nonlinear system (1), equation (9) can be iterated to calculate an approximation for $\boldsymbol{\phi}$ in the form of a sequence in powers of the residual \mathcal{R} . This leads to the sequence $\boldsymbol{\phi}^{(n)}(t)$, with $\boldsymbol{\phi}^{(0)}(t) = \boldsymbol{\psi}$. By subsequently taking the convolution product with $B(t)$, approximate solutions $\mathbf{X}_\psi^{(n)}(t)$ to (1) can be obtained. Explicitly, the iteration for these approximants reads

$$\mathbf{X}_\psi^{(n)}(t) = (B * \boldsymbol{\phi}^{(n)})(t) = \mathbf{X}_\psi^{(0)}(t) + \left(B * \mathcal{R} \mathbf{X}_\psi^{(n-1)} \right) (t), \quad (10)$$

where

$$\mathbf{X}_\psi^{(0)}(t) = (B * \boldsymbol{\phi}^{(0)})(t) = (B * \boldsymbol{\psi})(t) \quad (11)$$

is the zeroth approximant, which is the convolution product of the linear problem. We now turn to applying the BLUES iteration procedure to the SIRS epidemiological model for the spreading of infectious diseases.

III. THE SIRS MODEL WITH CONSTANT VACCINATION

The SIRS model consists of a group of susceptible (S), infected (I) and recovered/immune (R) (human) individuals. The total population $N = S + I + R$ can grow by virtue of a (constant) birth rate π and decay through natural deaths at a rate μ . At birth, the individuals are vaccinated with probability p and consequently acquire immunity, effectively adding up to the group of immune individuals. The remainder of the new births are added to the susceptible group with probability $1 - p$. Through contact with infected individuals, a person can become infected, following a mass-action law βSI with force of infection βI . The infected can recover with rate γ , acquiring (temporary) immunity and moving to the group of recovered or immune individuals. Finally, immunity can be lost with rate ξ , whereby recovered individuals move back to the susceptible population. Fig.1 illustrates these different processes in a flow diagram. We assume that all system parameters and populations are positive, and $0 \leq p \leq 1$.

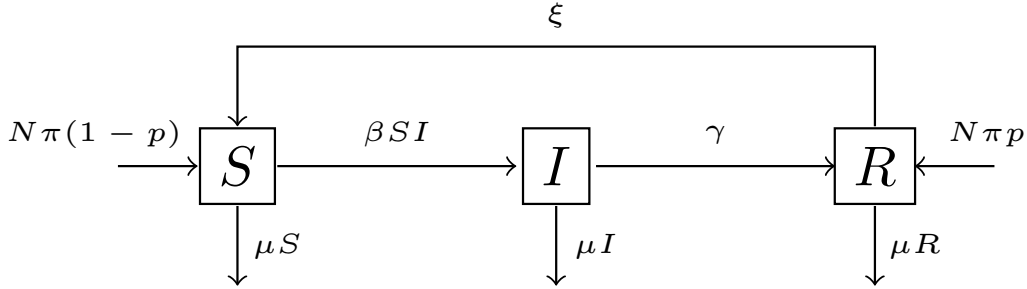


Figure 1: SIRS model with vaccination, immunity loss, births and natural deaths.

The interactions between the different populations can be described by the following nonlinear system of DEs, in which the prime denotes derivative w.r.t. time,

$$S'(t) = N(t)\pi(1-p) - \beta \frac{S(t)I(t)}{N(t)} - \mu S(t) + \xi R(t) \quad (12a)$$

$$I'(t) = \beta \frac{S(t)I(t)}{N(t)} - (\gamma + \mu)I(t) \quad (12b)$$

$$R'(t) = N(t)\pi p + \gamma I(t) - (\mu + \xi)R(t). \quad (12c)$$

The time evolution of the total population $N = S + I + R$ can be found by adding (12a)-(12c)

$$N'(t) = (\pi - \mu)N(t), \quad (13)$$

which indicates that the population is not constant. $N(t)$ is a nondecreasing function of t when the birth rate is higher than or equal to the death rate, $\pi \geq \mu$. To study the relative importance of the various population fractions, we scale S, I and R by the total population N , i.e., $s(t) = S(t)/N(t)$, $i(t) = I(t)/N(t)$ and $r(t) = R(t)/N(t)$. This transforms the system (12) into the following system for the fractions,

$$s'(t) = \pi(1 - p) - \beta s(t)i(t) - \pi s(t) + \xi r(t) \quad (14a)$$

$$i'(t) = \beta s(t)i(t) - (\gamma + \pi)i(t) \quad (14b)$$

$$r'(t) = \pi p + \gamma i(t) - (\pi + \xi)r(t), \quad (14c)$$

where $s(t) + i(t) + r(t) = 1$, $\forall t \geq 0$. Note that μ is eliminated by this transformation. By using the constraint on the population fractions, we can eliminate $r(t)$ and study the “two-dimensional” invariant system

$$s'(t) = \pi(1 - p) - \beta s(t)i(t) - (\pi + \xi)s(t) - \xi i(t) + \xi \quad (15a)$$

$$i'(t) = \beta s(t)i(t) - (\pi + \gamma)i(t). \quad (15b)$$

From a stability analysis performed in appendix A, we deduce that the above system has two globally stable fixed points, which are known exactly: a disease-free equilibrium (A1a) $\varepsilon_0 \equiv (s_0^*, i_0^*) = \left(1 - \frac{\pi p}{\pi + \xi}, 0\right)$ for which the disease is eradicated and an endemic equilibrium (A1b) $\varepsilon_e \equiv (s_e^*, i_e^*) = \left(\frac{\pi + \gamma}{\beta}, \frac{\beta((1-p)\pi + \xi) - (\gamma + \pi)(\xi + \pi)}{\beta(\gamma + \pi + \xi)}\right)$ for which the disease persists and keeps circulating through the population. The final state of the system is characterised by the *vaccination reproduction number* R_V

$$R_V = \frac{\beta((1-p)\pi + \xi)}{(\pi + \gamma)(\pi + \xi)}, \quad (16)$$

which represents the average number of susceptible individuals which are infected by one sick individual during their infectuous period, while a vaccination program is in long-time use [15].

Obviously, the endemic equilibrium ε_e can only exist when $s_e^* < 1$ and $i_e^* > 0$ which means that the vaccination reproduction number must satisfy $R_V > 1$. The disease will be fully eradicated whenever the disease-free equilibrium is the only possible stable fixed point and the endemic equilibrium does not exist. This happens when the vaccination probability p is higher than the critical vaccination threshold p_c , which can be inferred from equation

(16) by setting $R_V = 1$,

$$p_c = \left(\frac{\xi}{\pi} + 1 \right) \left(1 - \frac{\gamma + \pi}{\beta} \right). \quad (17)$$

Note that p_c may exceed unity, whereas p cannot.

IV. BLUES FUNCTION METHOD FOR THE SIRS MODEL

To find solutions of the system (15), we can write it as a nonlinear matrix equation, as was demonstrated in section II, i.e.,

$$\mathcal{N}_t \mathbf{X}(t) = \boldsymbol{\psi}(t) \quad (18)$$

with $\mathbf{X}(t)$ the vector of solutions,

$$\mathbf{X}(t) = \begin{pmatrix} s(t) \\ i(t) \end{pmatrix} \quad (19)$$

and with source vector $\boldsymbol{\psi}(t) = \boldsymbol{\chi}\Theta(t) + \mathbf{C}\delta(t)$, with $\boldsymbol{\chi}$ the (time-independent) vector of external sources and \mathbf{C} the vector of initial conditions, i.e.,

$$\boldsymbol{\chi} = \begin{pmatrix} \chi_s \\ \chi_i \end{pmatrix} \quad \text{and} \quad \mathbf{C} = \begin{pmatrix} s_0 \\ i_0 \end{pmatrix} \equiv \begin{pmatrix} s(0) \\ i(0) \end{pmatrix}. \quad (20)$$

Note that we have included the initial conditions in the source $\boldsymbol{\psi}$ by multiplication with a Dirac point source located at $t = 0$, as was explained in Section II.

Now we judiciously tailor the linear operator that is congruous with the asymptotic equilibrium, by rewriting the nonlinear term in (15) so that already the linear system captures the stable fixed point exactly. This is done by including the deviations of the population fractions from their equilibrium values in the (revised) nonlinear term, as follows,

$$s'(t) = \pi(1 - p) - \beta(s(t) - s^*)(i(t) - i^*) - (\pi + \xi - \beta i^*)s(t) - (\xi + \beta s^*)i(t) + \xi + \beta s^* i^* \quad (21a)$$

$$i'(t) = \beta(s(t) - s^*)(i(t) - i^*) - (\pi + \gamma - \beta s^*)i(t) + \beta i^* s(t) - \beta s^* i^*, \quad (21b)$$

where s^* and i^* are the elements of the fixed point vector $\epsilon = (s^*, i^*)$ which represents the equilibrium that is reached. This equilibrium depends uniquely on the value of R_V . Note that the refurbished nonlinear term vanishes at the fixed point and represents the product

of the fluctuations in susceptible and in infected fractions relative to the equilibrium values. This approach captures the correct asymptotic behaviour for long times provided the linear relaxation times for both $s(t)$ and $i(t)$ exist. This is the case for all $R_V \neq 1$. For $R_V = 1$ this strategy fails because $i(t)$ is then a marginal variable in the linear system since $i'(t) = 0$ at linear level, which precludes an approach to the fixed point. However, a different choice of linear operator will fix this problem. We will discuss the special (critical) case $R_V = 1$ separately.

With the calibration chosen as in (21) we proceed to identify the linear operator,

$$\mathcal{L}_t \mathbf{X} = \mathbf{X}_t - A\mathbf{X} = \boldsymbol{\chi}\Theta + \mathbf{C}\delta = \boldsymbol{\psi} \quad (22)$$

where the subscript t on \mathbf{X} denotes the time derivative, A is the matrix with elements,

$$A = \begin{pmatrix} -(\pi + \xi - \beta i^*) & -(\xi + \beta s^*) \\ \beta i^* & -(\pi + \gamma - \beta s^*) \end{pmatrix} \quad (23)$$

and $\boldsymbol{\chi}$ is the vector with elements

$$\boldsymbol{\chi} = \begin{pmatrix} \pi(1-p) + \xi + \beta s^* i^* \\ -\beta s^* i^* \end{pmatrix}. \quad (24)$$

The (nonlinear) residual operator \mathcal{R} applied to the solution vector \mathbf{X} then takes the form

$$\mathcal{R}\mathbf{X} = \begin{pmatrix} -\beta(s(t) - s^*)(i(t) - i^*) \\ \beta(s(t) - s^*)(i(t) - i^*) \end{pmatrix}. \quad (25)$$

Following the procedure outlined in Section II, we construct an iteration sequence (10) for the solution vector $\mathbf{X}(t)$, i.e.,

$$\mathbf{X}^{(n)}(t) = (B * \boldsymbol{\phi}^{(n)})(t) = \mathbf{X}^{(0)}(t) + (B * \mathcal{R}\mathbf{X}^{(n-1)})(t), \quad (26)$$

where $B(t)$ is taken to be the matrix Green function $G(t)$ for the linear problem defined through (22). This $G(t)$ can be found as the inverse of the fundamental matrix of the matrix of coefficients A or equivalently as the matrix exponential of tA multiplied by a step function, i.e.,

$$G(t) = e^{tA} \Theta(t). \quad (27)$$

For the disease-free equilibrium ($R_V < 1$) we obtain,

$$G(t) = \begin{pmatrix} e^{-(\pi+\xi)t} & \frac{\xi+(\pi+\gamma)R_V}{(\xi-\gamma)+(\pi+\gamma)R_V} (e^{-(\pi+\xi)t} - e^{-(\pi+\gamma)(1-R_V)t}) \\ 0 & e^{-(\pi+\gamma)(1-R_V)t} \end{pmatrix} \Theta(t). \quad (28)$$

In this (simple) case the Green function matrix is triangular, so that its eigenvalues are conspicuous on the main diagonal. These eigenvalues contain the essential “damping” by virtue of the decaying exponentials, with finite “linear relaxation times” $\tau_s = 1/(\pi + \xi)$ and $\tau_i = 1/((\pi + \gamma)(1 - R_V))$. Note that τ_i diverges for $R_V \uparrow 1$. In this limit the relaxation to the disease-free equilibrium becomes “nonlinear”. The damping (for $R_V < 1$) ensures that the long-time asymptotics of the approximants, calculated through convolution, are well behaved.

The general Green function matrix, appropriate for both disease-free and endemic equilibria, is more involved and reads,

$$G(t) = \frac{e^{-Lt/2}}{2M} \begin{pmatrix} Z_+ e^{\frac{Mt}{2}} + Z_- e^{-\frac{Mt}{2}} & 2 \left(e^{-\frac{Mt}{2}} - e^{\frac{Mt}{2}} \right) (\beta s^* + \xi) \\ 2 \left(e^{\frac{Mt}{2}} - e^{-\frac{Mt}{2}} \right) \beta i^* & Z_+ e^{-\frac{Mt}{2}} + Z_- e^{\frac{Mt}{2}} \end{pmatrix} \Theta(t), \quad (29)$$

with

$$\begin{aligned} Z_{\pm} &= M \pm K \\ K &= \gamma - \xi - \beta(s^* + i^*) \\ L &= \gamma + \xi + 2\pi - \beta(s^* - i^*) \\ M^2 &= \gamma^2 + [\beta(s^* - i^*) + \xi]^2 - 2\gamma(\gamma - K). \end{aligned} \quad (30)$$

The zeroth approximant (11) is the convolution of the matrix Green function with the source vector $\boldsymbol{\psi}(t)$, i.e.,

$$\mathbf{X}^{(0)}(t) = (G * \boldsymbol{\psi})(t) = \int_{\mathbb{R}} G(t - t') [\boldsymbol{\chi}\Theta(t') + \mathbf{C}\delta(t')] dt' \quad (31)$$

and results in the following expressions for the population fraction of susceptible and infected individuals, respectively,

$$\begin{aligned} s^{(0)}(t) &= \frac{i_0(\beta s^* + \xi)}{M} e^{-Lt/2} (e^{-Mt/2} - e^{Mt/2}) + \frac{s_0}{2M} e^{-Lt/2} (Z_- e^{-Mt/2} + Z_+ e^{Mt/2}) \\ &+ \frac{2\beta s^* i^* (\beta s^* + \xi)}{M} \left(\frac{(e^{-Lt/2} - e^{-Mt/2})}{L - M} - \frac{(e^{-Lt/2} - e^{Mt/2})}{L + M} \right) \\ &+ \frac{(\beta s^* i^* + \pi(1 - p) + \xi) e^{-Lt/2}}{M} \left(\frac{Z_- (e^{Lt/2} - e^{-Mt/2})}{L + M} \right) \\ &+ \frac{(\beta s^* i^* + \pi(1 - p) + \xi) e^{-Lt/2}}{M} \left(\frac{Z_+ (e^{Lt/2} - e^{Mt/2})}{L - M} \right) \end{aligned} \quad (32)$$

$$\begin{aligned}
i^{(0)}(t) = & \frac{s_0 \beta i^*}{M} e^{-Lt/2} (e^{Mt/2} - e^{-Mt/2}) + \frac{i_0}{2M} e^{-Lt/2} (Z_- e^{Mt/2} + Z_+ e^{-Mt/2}) \\
& - \frac{2\beta i^* (\beta s^* i^* + (1-p)\pi + \xi) e^{Mt/2}}{M} \left(\frac{(e^{-Lt/2} - e^{-Mt/2})}{L-M} \right) \\
& + \frac{2\beta i^* (\beta s^* i^* + (1-p)\pi + \xi) e^{Mt/2}}{M} \left(\frac{(e^{-Lt/2} - e^{-Mt/2}) e^{-Mt}}{L+M} \right) \\
& - \frac{\beta s^* i^*}{M} e^{-Lt/2} \left(\frac{Z_- (e^{Lt/2} - e^{Mt/2})}{L-M} + \frac{Z_+ (e^{Lt/2} - e^{-Mt/2})}{L+M} \right). \tag{33}
\end{aligned}$$

Upon inspection of this and higher approximants (not reported analytically here) we infer that all BLUES approximants, regardless of the number of iterations ($n \geq 0$), are qualitatively correct asymptotically, for all $R_V \neq 1$, in that they converge exponentially rapidly towards the exact fixed point values for long times, in contrast with the other methods which yield divergencies.

We proceed to compare graphically the solution of the SIRS model calculated with the BLUES method with a precise numerical solution and with approximate solutions obtained by the ADM, the VIM, or homotopy perturbation method (HPM). In Table I the parameters are shown for three different cases, together with the values for the vaccination reproduction number R_V and critical vaccination threshold p_c . Depending on the value of R_V , we indicate in the last column of Table I the equilibrium attained by the system.

Table I: Parameters and corresponding equilibria for the 3 studied cases in the SIRS model. The vaccination reproduction number R_V and critical vaccination threshold p_c are also shown. Note that the latter exceeds unity in Case 2, which is physically equivalent to setting it equal to unity. For all cases $s_0 = 0.8$, $i_0 = 0.2$, $\beta = 0.8$, $\gamma = 0.03$ and $\pi = 0.4$.

	ξ	p	p_c	R_V	Equilibrium
Case 1	0.1	0.9	0.5781	0.5209	$\varepsilon_0 = (0.28, 0)$
Case 2	0.5	0.9	$1.0406 \implies 1$	1.1163	$\varepsilon_e = (0.5375, 0.0605)$
Case 3	0.1	0.5781	0.5781	1	$\varepsilon_0 = (0.5375, 0)$

Case 1: small loss of immunity and high vaccination probability.

As a preliminary remark, we mention that for $\xi = 0$ (no loss of immunity) the SIRS reduces to a SIR model with vaccination, which was treated earlier in [6, 7] by means of the ADM, HPM and VIM. Here we consider the SIRS model in which the protection offered by vaccination or post-disease immunity is lost with a small probability $\xi = 0.1$ after some time. When the vaccination probability $p = 0.9$ is higher than the critical vaccination threshold $p_c = 0.5781$, the disease will eventually die out and the system will reach the stable disease-free equilibrium for which $i \rightarrow 0$ and $s \rightarrow 0.28$. This is shown in Fig. 2. As we already discussed the BLUES method is accurate and captures the fixed-point values (A1a) of (s_0^*, i_0^*) in the equilibrium exactly. We remark that the approximants generated by the ADM, VIM and HPM diverge uncontrollably for longer times while the BLUES approximants converge globally for all $t \geq 0$ and in every iteration.

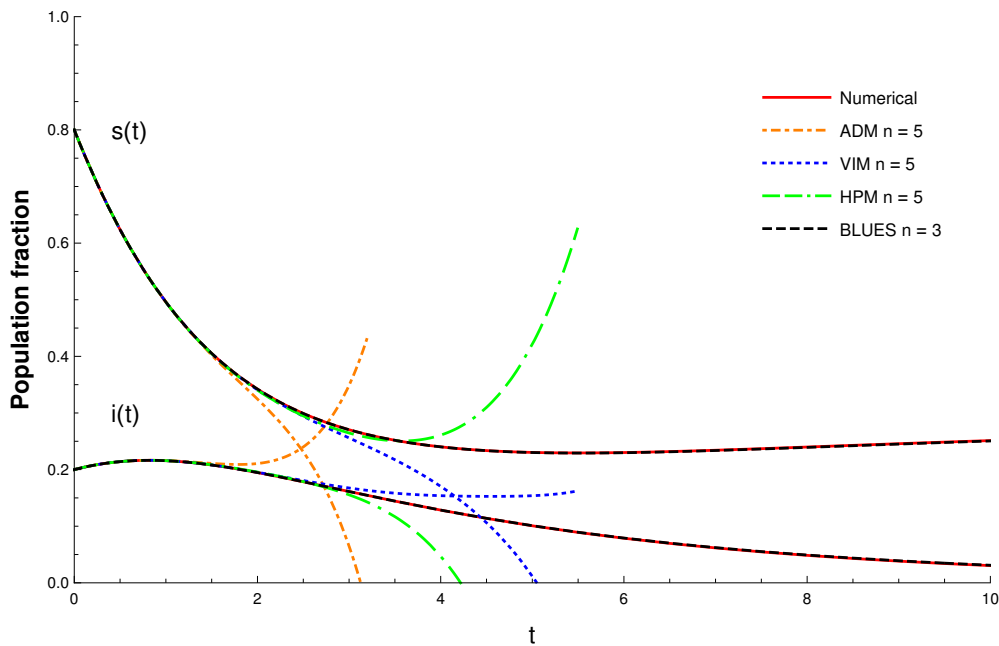


Figure 2: Comparison between the numerical solution (red line), the fifth-order ADM (orange dot-dashed line), the fifth-order VIM (blue dotted line), the fifth-order HPM (green dot-dash-dashed line) and the third BLUES approximant (black, dashed line) for Case 1 of the SIRS model: $\xi = 0.1$ and $p = 0.9$. In this case the disease-free equilibrium is reached for $t \rightarrow \infty$. Note that the numerical solution and the BLUES approximant are indistinguishable at this resolution.

We also compare the BLUES approximants for different numbers of iteration and notice that they converge rapidly towards the numerical solution. This is shown in Fig. 3.

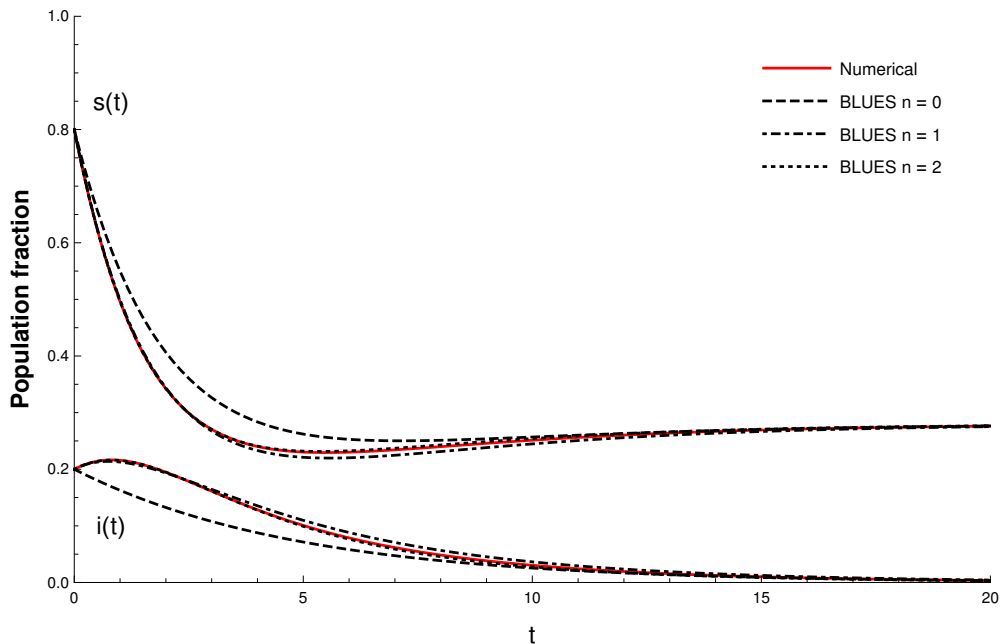


Figure 3: Comparison and convergence of BLUES approximants after zero (dashed line), one (dot-dashed line) and two (dotted line) iterations. The numerical solution is also shown (red line). This figure is for Case 1 of the SIRS model: $\xi = 0.1$ and $p = 0.9$. The convergence is global and all approximants (for all n) attain the exact fixed point values for $t \rightarrow \infty$. The asymptotic behavior for long times is an exponential decay. Note that the numerical solution and the second BLUES approximant are indistinguishable at this resolution.

Case 2: high loss of immunity and high vaccination probability.

As a second example, we consider the case in which immunity is more easily lost ($\xi = 0.5$) and the population is putting in an effort to vaccinate a larger number of people ($p = 0.9$). We can deduce from the critical vaccination probability $p_c = 1.0406$ in Table I that even when all civilians are vaccinated, immunity is lost so quickly that the population always reaches the endemic equilibrium and the disease cannot be eradicated. The result of a comparison between the ADM, VIM, HPM and BLUES methods is shown in Fig. 4. We also compare the BLUES approximants for different numbers of iteration and observe that

they converge rapidly towards the numerical solution. This is shown in Fig. 5.

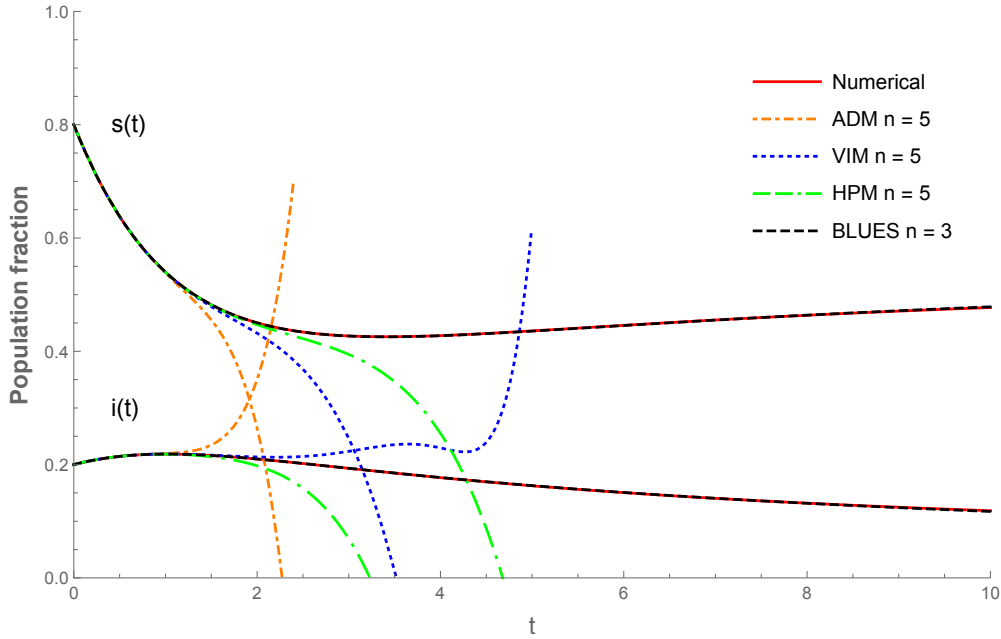


Figure 4: Comparison between the numerical solution (red line), the fifth-order ADM, VIM, and HPM approximants (respectively, blue dotted, orange dot-dashed and green dot-dash-dashed lines) and the third BLUES approximant (black, dashed line) for Case 2 of the SIRS model: $\xi = 0.5$ and $p = 0.9$. In this case the endemic equilibrium is reached for $t \rightarrow \infty$. Note that the numerical solution and the BLUES approximant are indistinguishable at this resolution.

Case 3: nonlinear relaxation at the dynamical critical point.

In this third case, we study the dynamical criticality at $R_V = 1$. The population still reaches the disease-free equilibrium asymptotically, but much more slowly since in the limit $R_V \uparrow 1$ the linear relaxation time diverges. The “linear” exponential relaxation is replaced by a “nonlinear” algebraic one, with leading behaviour for long times proportional to $1/t$. This can be inferred exactly from an analysis of the asymptotic behaviour of the system of DEs (21), which at $R_V = 1$ reduces to,

$$s'(t) = \pi(1 - p) - \beta(s(t) - s^*)i(t) - (\pi + \xi)s(t) - (\xi + \beta s^*)i(t) + \xi \quad (34a)$$

$$i'(t) = \beta(s(t) - s^*)i(t), \quad (34b)$$

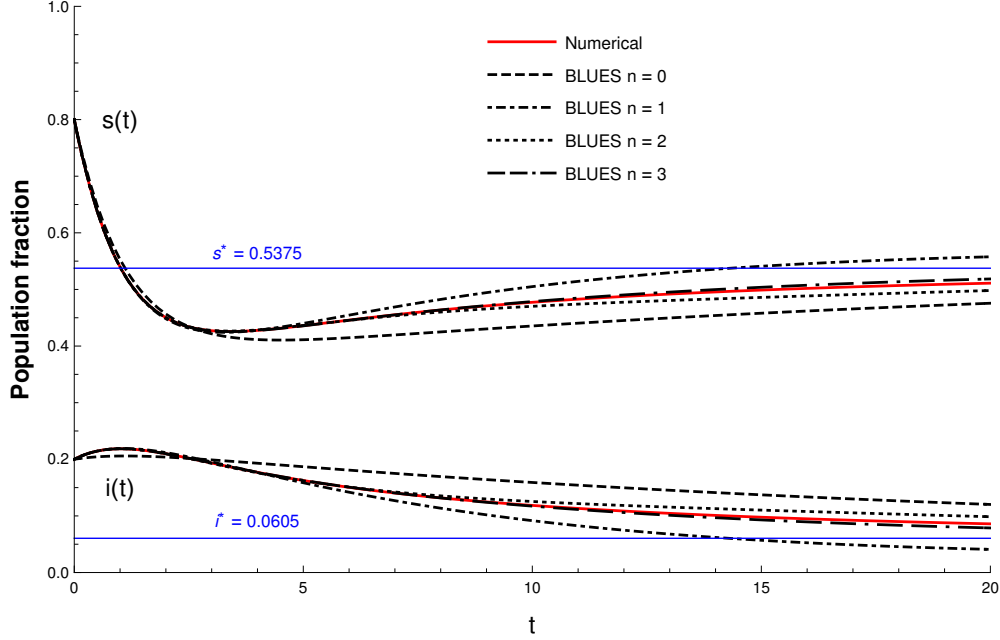


Figure 5: Comparison and convergence of BLUES approximants after zero (dashed line), one (dot-dashed line), two (dotted line) and three (dot-dash-dashed line) iterations. The numerical solution is also shown (red line). This figure is for Case 2 of the SIRS model: $\xi = 0.5$ and $p = 0.9$. The convergence is global and all approximants (for all n) attain the exact fixed point values for $t \rightarrow \infty$ indicated by the horizontal blue lines. The asymptotic behaviour for long times is an exponential decay.

with, in this special case, $s^* = s_0^* = s_e^*$. Inspection of these DEs allows us to establish that the leading asymptotic behavior is a $1/t$ power-law decay towards the fixed point,

$$s(t) = s^* - \frac{1}{\beta t} + \mathcal{O}(t^{-2}) \quad (35a)$$

$$i(t) = \frac{\pi + \xi}{\pi + \xi + \gamma} \frac{1}{\beta t} + \mathcal{O}(t^{-2}), \quad (35b)$$

A successful application of the BLUES function method is possible if we acknowledge that we must reconsider the decomposition of the problem into a nonlinear and a linear part. This is necessary in view of the divergence of the “linear relaxation time” $\tau_i = 1/((\pi + \gamma)(1 - R_V))$ and the concomitant vanishing of one of the eigenvalues of the linear matrix A given by the triangular form (23), which is appropriate for the disease-free equilibrium. If we stick to this choice there is not enough “damping” in the convolution products that govern the iteration procedure (10) and the approximants diverge, similarly to what routinely happens in the ADM, the VIM and HPM. However, we can recalibrate the linear operator so that both

eigenvalues are non-zero and nevertheless the correct (disease-free) fixed point is reached for $t \rightarrow \infty$. This is achieved simply by retaining the original nonlinear term in (15) without refurbishing it. The matrix of coefficients A of the linear operator and the residual operator hence become, respectively,

$$A = \begin{pmatrix} -\pi - \xi & -\xi \\ 0 & -\pi - \gamma \end{pmatrix} \quad (36)$$

and

$$\mathcal{R}\mathbf{X} = \begin{pmatrix} -\beta s(t)i(t) \\ \beta s(t)i(t) \end{pmatrix}. \quad (37)$$

This linear system ensures a correct approach to the fixed point for $R_V = 1$ and is a good starting point for the BLUES iteration in this dynamical critical point. We recover global convergence to the numerically exact solution, but at a slower pace than in the noncritical case because the approximants decay exponentially fast for long times, whereas the exact solution features an algebraic decay. The characteristic time of the leading exponentials is constant for all approximants but the amplitude, sign and polynomial prefactors vary as the iteration number n increases. This is how the iteration sequence attempts to approximate an algebraic decay in the limit $n \rightarrow \infty$ (see Fig.7).

Time of the infection peak

We now calculate the (dimensionless) time $t = \hat{t}$ at which the peak of the infection occurs from the BLUES approximants and compare with the numerically precise values. At the infection peak, $i'(\hat{t}) = 0$, and hence, using equation (15b), we deduce that $s(\hat{t}) = (\gamma + \pi)/\beta$. So, instead of trying to solve $i'(\hat{t}) = 0$ directly, we can find \hat{t} from the susceptible population fraction. The results are shown in Fig. 8. The BLUES function method accurately captures the infection peak time, both for the disease-free and the endemic equilibria.

V. CONCLUSIONS

In this paper we have presented a twofold advance. The first consists of qualitative progress in accuracy and convergence of analytic approximations to solutions of the SIRS

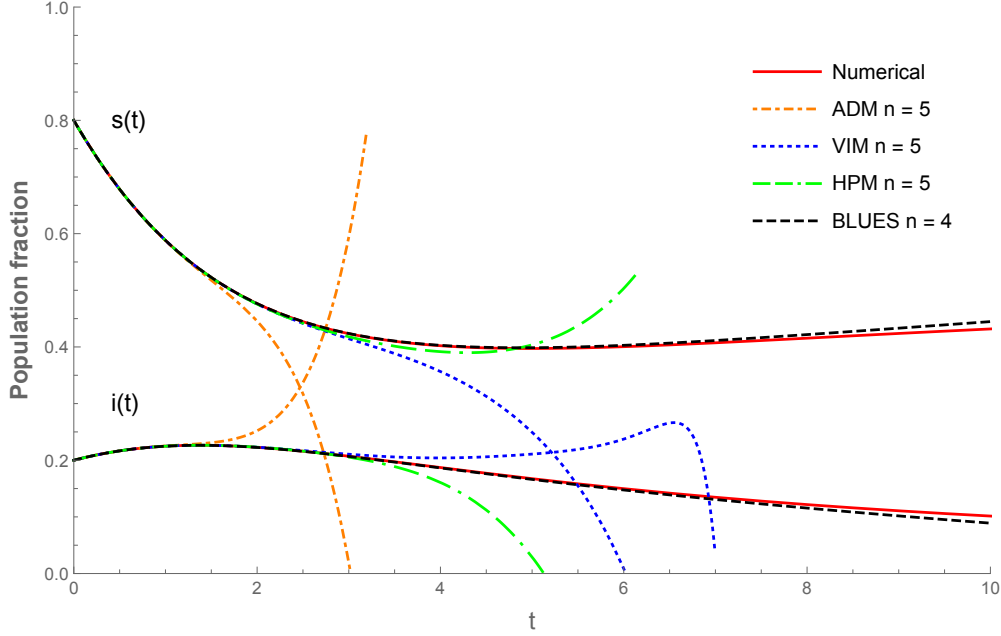


Figure 6: Comparison between the numerical solution (red line), the fifth-order ADM, VIM, and HPM approximants (respectively, blue dotted, orange dot-dashed and green dot-dash-dashed lines) and the fourth BLUES approximant (black, dashed line). This figure is for Case 3 of the SIRS model: a critical point with $\xi = 0.1$ and $p = p_c = 0.5781$, implying $R_V = 1$. Note that the BLUES approximant is initially very close to, but later deviates somewhat from the numerical solution. This is due to the difference in the type of asymptotic decay, which is conspicuous in Fig.7.

model for epidemic spreading. The second is concerned with a technical and methodological refinement, being the development of a *matrix* BLUES function method for *coupled* nonlinear ordinary differential equations.

We have shown that the method can be applied to obtain analytic approximants for the SIRS model with vital dynamics, constant vaccination strategy and loss of immunity. We have made a detailed comparison of the iteration procedure with the Adomian decomposition method, the variational iteration method and homotopy perturbation method. It is found that all methods succeed in approximating the (numerically) exact solutions locally and, for the BLUES function method, also globally. The BLUES method generates approximants with a higher accuracy, for the same number of iterations performed, and, moreover, is able to capture the asymptotic behaviour of the solutions for long times in both the disease-free and endemic equilibria.

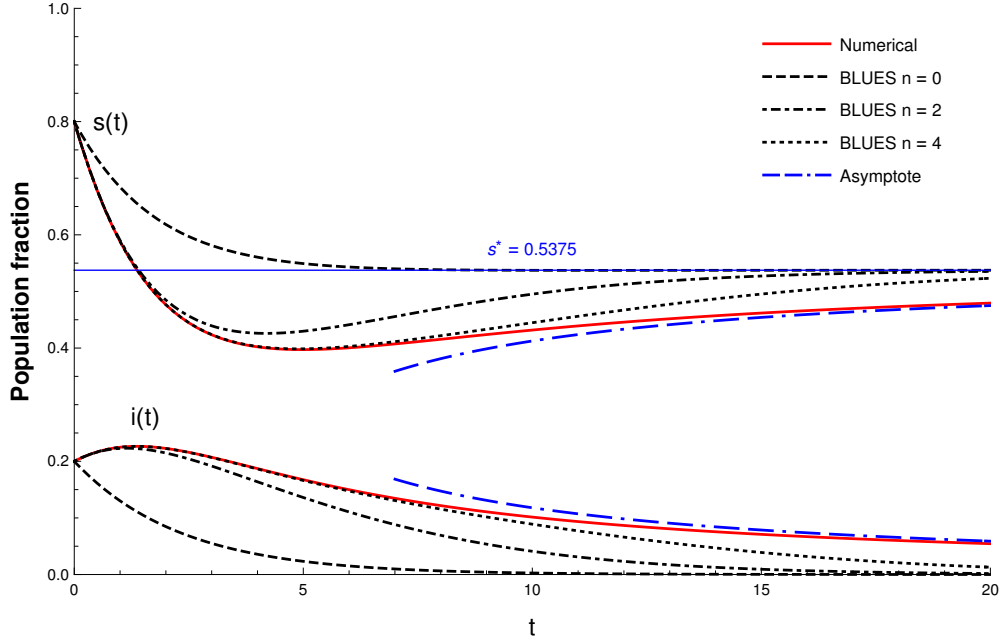


Figure 7: Comparison and convergence of the BLUES approximants after zero (dashed line), two (dot-dashed line) and four (dotted line) iterations. The numerical solution is also shown (red line) together with its exact asymptotic behaviour (a power-law decay). This figure is for Case 3 of the SIRS model: a critical point with $\xi = 0.1$ and $p = p_c = 0.5781$, implying $R_V = 1$. The convergence is global and all approximants (for all n) attain the exact fixed point values for $t \rightarrow \infty$. However, the asymptotic behaviour of the exact solution for long times is an algebraic decay, whereas the BLUES approximants feature an exponential decay.

A prominent strength of the BLUES function method is that it permits the user to tailor judiciously the linear part of the operator so that its Green function contains just enough damping to temper, in each iteration, its convolution with the emergent source in order to capture the correct asymptotics of the solution of the nonlinear problem. In other words, for an optimal choice of the linear part and its associated Green function, the BLUES iterations converge globally to the numerically exact solution of the problem. For a suboptimal choice of the linear part local convergence can still be achieved, but in that case the advantages over other methods are less pronounced. An illustration of an optimal and suboptimal choice of linear operator has been presented in the case of the dynamical critical point of the SIRS model.

With the recent ongoing COVID-19 pandemic, it has become clear that mathematical

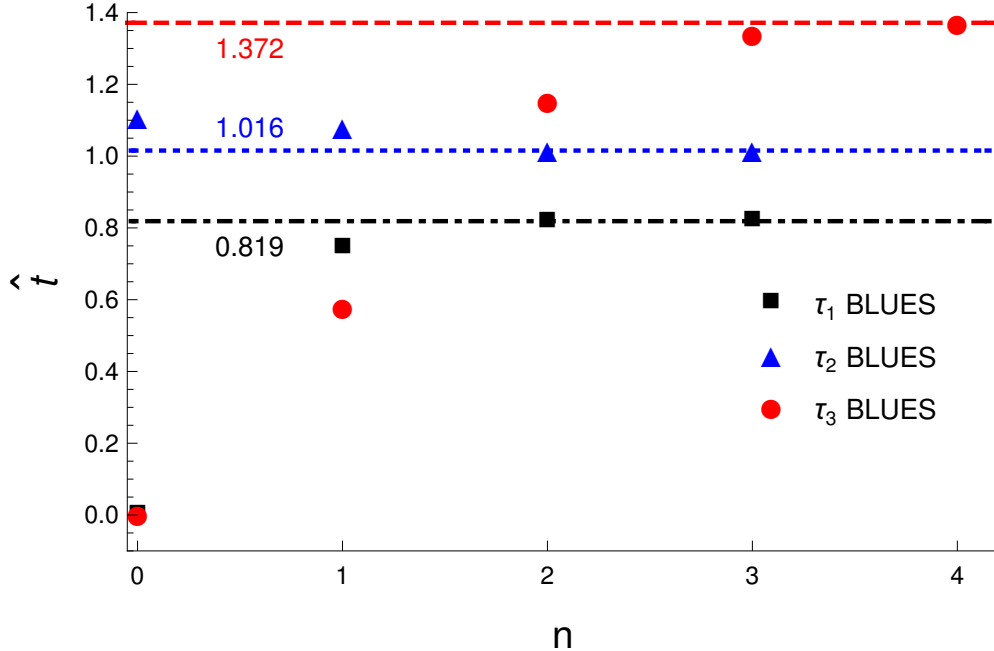


Figure 8: Comparison between the numerically precise (dimensionless) time of the infection peak \hat{t} in the SIRS model and the values calculated using the n th BLUES approximants ($n = 0, 1, 2, 3, 4$) for Case 1 (red dashed line and red circles), Case 2 (black dot-dashed line and black squares) and Case 3 (blue dotted line and blue triangles).

modelling of epidemic processes is crucial to understanding (and possibly also predicting) the evolution of these viral outbreaks. None of the epidemiological models have exact closed-form solutions, with the exception of the SIS model [16] in which no immunity is possible and individuals return to the susceptible contingent once they recover from the infection. Hence, approximate solutions are needed to assess the impact of the different model parameters without resorting to brute force methods such as numerical simulation. This paper has aimed at showing that the BLUES method is a good candidate for obtaining such approximate analytic solutions. This application of the method to coupled ODEs paves the way for applications to more involved systems such as coupled PDEs [12, 17], for instance.

Appendix A: Stability analysis

The system (15) has two fixed points that can be found by a fixed-point analysis which reveals a disease-free equilibrium ε_0 in which the disease has died out, and an endemic equilibrium ε_e in which the infected population density reaches a nonzero asymptotic value,

i.e.,

$$\varepsilon_0 = (s_0^*, i_0^*) = \left(1 - \frac{\pi p}{\pi + \xi}, 0\right) \quad (\text{A1a})$$

$$\varepsilon_e = (s_e^*, i_e^*) = \left(\frac{\pi + \gamma}{\beta}, \frac{\beta((1-p)\pi + \xi) - (\gamma + \pi)(\xi + \pi)}{\beta(\gamma + \pi + \xi)}\right). \quad (\text{A1b})$$

Note that the disease-free equilibrium ε_0 is independent of the average contact rate β . The endemic equilibrium (A1b) can now be simplified to

$$\varepsilon_e = (s_e^*, i_e^*) = \left(\left(1 - \frac{\pi p}{\pi + \xi}\right) \frac{1}{R_V^{(\text{SIRS})}}, \frac{(1-p)\pi + \xi}{\gamma + \pi + \xi} \left(1 - \frac{1}{R_V^{(\text{SIRS})}}\right)\right). \quad (\text{A2})$$

These two fixed points are globally stable. This means that for an arbitrary initial condition in the si -plane, the trajectory will converge onto one of these two fixed points. Which fixed point is reached depends on the system parameters π, β, γ, ξ and p .

The global asymptotic stability for the endemic equilibrium can be proven as follows. First note that the positive quadrant \mathbb{R}_+^2 of the si -plane is not an invariant set of the system (15), i.e., when $s(t) = 0$ then $s'(t) < 0$ for all values $i(t) > (\pi(1-p) + \xi)/\xi$. This can be resolved by shifting (s, i) to (Σ, i) , where

$$\Sigma(t) = s(t) + \frac{\xi}{\beta}. \quad (\text{A3})$$

Hence, the shifted system becomes

$$\Sigma'(t) = \pi(1-p) - \beta\Sigma(t)i(t) - (\pi + \xi)\Sigma(t) + \frac{\xi}{\beta}(\xi + \pi) + \xi \quad (\text{A4a})$$

$$i'(t) = \beta\Sigma(t)i(t) - (\gamma + \pi + \xi)i(t). \quad (\text{A4b})$$

It is now easy to see for $\Sigma(t) = 0$, now $\Sigma'(t) \geq 0$ for all values of $i(t)$. By shifting the system, the endemic equilibrium coordinates change as follows

$$(\Sigma_e^*, i_e^*) = \left(\frac{\pi + \gamma + \xi}{\beta}, \frac{\pi((1-p)\beta - \gamma - \pi) + \xi(\beta - \gamma - \pi)}{\beta(\pi + \gamma + \xi)}\right). \quad (\text{A5})$$

All global properties of the system remain invariant under the shifting of the coordinates, so we can now try to find a Lyapunov function $V(\Sigma, i)$ to prove global asymptotic stability of the endemic fixed point (A5) of the shifted system (A4) and hence also of the original system (15). We can choose the following Lyapunov function [18]

$$V(\Sigma, i) = \Sigma_e^* \left(\frac{\Sigma}{\Sigma_e^*} - \ln \frac{\Sigma}{\Sigma_e^*}\right) + i_e^* \left(\frac{i}{i_e^*} - \ln \frac{i}{i_e^*}\right) \quad (\text{A6})$$

with time derivative

$$\begin{aligned} V'(\Sigma, i) &= \frac{\partial V}{\partial \Sigma} \Sigma'(t) + \frac{\partial V}{\partial i} i'(t) \\ &= \left(1 - \frac{\Sigma_e^*}{\Sigma(t)}\right) \Sigma'(t) + \left(1 - \frac{i_e^*}{i(t)}\right) i'(t). \end{aligned} \quad (\text{A7})$$

Now, from (A4a) and (A4b) it is clear that for the endemic equilibrium the following holds

$$\begin{aligned} \beta \Sigma_e^* i_e^* &= \pi(1-p) - (\pi + \xi) \Sigma_e^* + \frac{\xi}{\beta} (\xi + \pi) + \xi \\ &= (\gamma + \pi + \xi) i_e^*. \end{aligned} \quad (\text{A8})$$

Substituting this property into (A7) and simplifying gives after some algebra

$$\begin{aligned} V'(\Sigma, i) &= \left(1 - \frac{\Sigma_e^*}{\Sigma(t)}\right) \Sigma'(t) + \left(1 - \frac{i_e^*}{i(t)}\right) i'(t) \\ &= - \left(\pi(1-p) + \frac{\xi}{\beta} (\xi + \pi) + \xi \right) \left(\frac{\Sigma(t)}{\Sigma_e^*} \right) \left(1 - \frac{\Sigma_e^*}{\Sigma(t)} \right)^2 \\ &\leq 0, \end{aligned} \quad (\text{A9})$$

for all values of $\Sigma, i \geq 0$. This concludes the proof that the endemic equilibrium is globally asymptotically stable. Proving the global stability of the disease-free fixed point is now trivial. One can repeat the previous calculations with the Lyapunov function

$$V(\Sigma, i) = \Sigma_0^* \left(\frac{\Sigma}{\Sigma_0^*} - \ln \frac{\Sigma}{\Sigma_0^*} \right) + i, \quad (\text{A10})$$

which is the same as (A6) with now Σ_0^* instead of Σ_e^* and $i_e^* \rightarrow 0$.

-
- [1] G. Adomian, *Solving Frontier Problems of Physics: The Decomposition Method*, 1st ed., Fundamental Theories of Physics, Vol. 60 (Springer Netherlands, 1994).
 - [2] G. Adomian, "A review of the decomposition method and some recent results for nonlinear equations," *Math. Comput. Model.* **13**, 17 – 43 (1990).
 - [3] J.-H. He, "Variational iteration method – Some recent results and new interpretations," *J. Comput. Appl. Math.* **207**, 3 – 17 (2007).
 - [4] J.-H. He, "Homotopy perturbation technique," *Comput. Methods Appl. Mech. Eng.* **178**, 257–262 (1999).
 - [5] W. O. Kermack and A. G. McKendrick, "A contribution to the mathematical theory of epidemics," *Proc. R. Soc. Lond. A* **115**, 700–721 (1927).

- [6] O. Makinde, “Adomian decomposition approach to a SIR epidemic model with constant vaccination strategy,” *Appl. Math. Comput.* **184**, 842 – 848 (2007).
- [7] A. R. Ghotbi, A. Barari, M. Omidvar, and G. Domairry, “Application of homotopy perturbation and variational iteration methods to SIR epidemic model,” *J. Mech. Med. Biol* **11**, 149–161 (2011).
- [8] S. Mungkasi, “Variational iteration and successive approximation methods for a SIR epidemic model with constant vaccination strategy,” *Appl. Math. Model.* **90**, 1 – 10 (2021).
- [9] J. O. Indekeu and K. K. Müller-Nedebock, “BLUES function method in computational physics,” *J. Phys. A-Math. Theor.* **51**, 165201 (2018).
- [10] J. Berx and J. O. Indekeu, “Analytic iteration procedure for solitons and traveling wavefronts with sources,” *J. Phys. A-Math. Theor.* **52**, 38LT01 (2019).
- [11] J. Berx and J. O. Indekeu, “BLUES iteration applied to nonlinear ordinary differential equations for wave propagation and heat transfer,” *J. Phys. A- Math. Theor.* **54**, 025702 (2020).
- [12] J. Berx and J. O. Indekeu, “Analytic approximants for interface growth under shear from the blues function method applied to partial differential equations,” (2021), arXiv:2103.08356 [physics.comp-ph].
- [13] V. V. Zozulya, “Green’s matrices for the BVP for the system of ODE of the first order: applications to the beam theories,” *Arch. Appl. Mech* **87**, 1605–1627 (2017).
- [14] S. K. Godunov, *Ordinary Differential Equations with Constant Coefficients*, Translations of mathematical monographs, Vol. 169 (American Mathematical Society, 1997).
- [15] P. van den Driessche, “Reproduction numbers of infectious disease models,” *Infect. Dis. Model.* **2**, 288 – 303 (2017).
- [16] H. W. Hethcote, “Three basic epidemiological models,” in *Applied Mathematical Ecology* (Springer Berlin Heidelberg, 1989) pp. 119–144.
- [17] J. M. Horowitz and M. Kardar, “Bacterial range expansions on a growing front: Roughness, fixation, and directed percolation,” *Phys. Rev. E* **99**, 042134 (2019).
- [18] A. Korobeinikov and G. Wake, “Lyapunov functions and global stability for SIR, SIRS, and SIS epidemiological models,” *Appl. Math. Lett.* **15**, 955 – 960 (2002).